Pump-probe spectroscopy in degenerate two-level atoms with arbitrarily strong fields

T. Zigdon, A. D. Wilson-Gordon, and H. Friedmann
Department of Chemistry, Bar-Ilan University, Ramat Gan 52900, Israel
(Received 24 December 2007; published 19 March 2008)

We study the pump and probe absorption spectra, as a function of the probe detuning, in a degenerate two-level atomic system, for the case where the probe intensity is high enough to affect the pump absorption. The theory is valid for any $F_g \rightarrow F_e$ alkali-metal transition interacting with an arbitrarily intense pump and probe (with general Rabi frequencies $\Omega_{1,2}$) which are perpendicularly polarized with either $\sigma_{\pm}$ or π polarization. We have constructed a computer program that can calculate the spectra without requiring one to write out the Bloch equations explicitly. We show that, when the pump is $\sigma_{\pm}$ polarized and the probe π polarized, or vice versa, the pump and probe absorptions depend on the Zeeman coherences between the nearest-neighboring ground or excited Zeeman sublevels, whereas when the pump is σ_+ polarized and the probe σ_- polarized, or vice versa, the Zeeman coherences that directly determine the absorption are between next-nearest neighbors. We report calculations of the pump and probe absorption spectra for the cycling $F_g=2 \rightarrow F_e=3$ transition in the D_2 line of ^{87}Rb, interacting with a resonant σ_+-polarized pump and either a π- or a σ_-- polarized probe. The probe and pump absorption spectra are analyzed by considering the contributions that derive from the individual $m_g \rightarrow m_e$ transitions. We then show how these contributions depend on the ground- and excited-state populations and Zeeman coherences, and investigate the role played by transfer of coherence from the excited to the ground hyperfine state. We show that the pump and probe absorption spectra are mirror images of each other when $\Omega_1 \geq \Omega_2 > \Gamma$, and have the same behavior at line center and complementary behavior in the wings, when $\Omega_1 \geq \Omega_2 < \Gamma$ (Γ is the rate of spontaneous decay from F_e to F_g).

DOI: 10.1103/PhysRevA.77.033836 PACS number(s): 42.50.Gy, 42.50.Hz

I. INTRODUCTION

In this paper, we study the pump and probe absorption spectra, as a function of the probe detuning, in a degenerate two-level system, for the case where the probe intensity is high enough to affect the pump absorption. The effect of a moderately intense probe on the pump absorption spectrum has been studied theoretically for a closed two-level system [1], an open two-level system [2], and a four-level N system [3] that models electromagnetically induced absorption (EIA) [4,5] due to transfer of coherence (TOC) in an $F_g \rightarrow F_e=F_g+1$ atomic transition, interacting with perpendicularly polarized pump and probe fields [6,7]. The effect of the probe on the pump absorption and refraction spectra has been studied experimentally by Spani Molella *et al.* [8] for the interaction of the $F_g=4 \rightarrow F_e=5$ transition in an atomic beam of ^{133}Cs atoms with perpendicularly linearly polarized lasers. Krmpot *et al.* [9] have investigated the effect of the probe on the pump absorption spectrum in nondegenerate V-, Λ-, and N-shaped systems in warm ^{85}Rb atomic vapor. The theory presented here is valid for any $F_g \rightarrow F_e$ alkali-metal transition interacting with an arbitrarily intense pump and probe which are perpendicularly polarized with either $\sigma_{\pm}$ or π polarizations, and indeed our computer program can handle any of these transitions without the necessity to write out the Bloch equations explicitly. We show that, when the pump is $\sigma_{\pm}$ polarized and the probe π polarized, or vice versa, the pump and probe absorptions depend on the Zeeman coherences between the nearest-neighboring ground or excited Zeeman sublevels, whereas when the pump is σ_+ polarized and the probe σ_- polarized, or vice versa, the Zeeman coherences that directly determine the absorption are between next-nearest neighbors. In both cases, these coherences oscillate at the pump-probe frequency difference $\pm\delta$, and are themselves determined by higher-order coherences at frequencies $\pm n\delta$, $n>1$.

In particular, we use the theory to calculate the pump and probe absorption spectra for the degenerate $F_g=2 \rightarrow F_e=3$ transition in the D_2 line of ^{87}Rb, interacting with a resonant σ_+-polarized pump and either a π- or a σ_--polarized probe [see Figs. 1(a) and 1(b) for the energy-level schemes]. Assuming throughout that the pumping rate is greater than the ground-state decay, we show that, for both combinations of polarizations, the pump and probe absorption spectra are either mirror images of each other or have the same behavior at line center and complementary behavior in the wings. The latter behavior was observed by Spani Molella *et al.* [8] in Cs. Pump and probe absorption spectra with the same general behavior do not occur for either of these polarizations, but do occur for the case of a π-polarized pump and a $\sigma_{\pm}$ probe. This case will be discussed elsewhere.

For the case of perpendicularly polarized, weak pump and probe lasers, EIA has been shown to be due to TOC, via spontaneous emission, from the excited state to the ground state [6]. In our earlier work on EIA [7], we explained that the TOC that leads to EIA in degenerate systems can take place only when ground-state population trapping is incomplete, that is, when $F_e=F_g+1$. However, incomplete population trapping and hence TOC can also be achieved when $F_e=F_g-1$, with $F_g>1$, when the degeneracy is lifted by applying a weak magnetic field. We used this fact to explain the origin of EIA in the probe spectrum of a multitripod system [10], formed when a σ-polarized pump and a tunable π-polarized probe laser interact with an $F_g \rightarrow F_e=F_g-1$ transition, in the presence of a weak magnetic field. We also showed there that the probe spectrum for a noncycling tran-

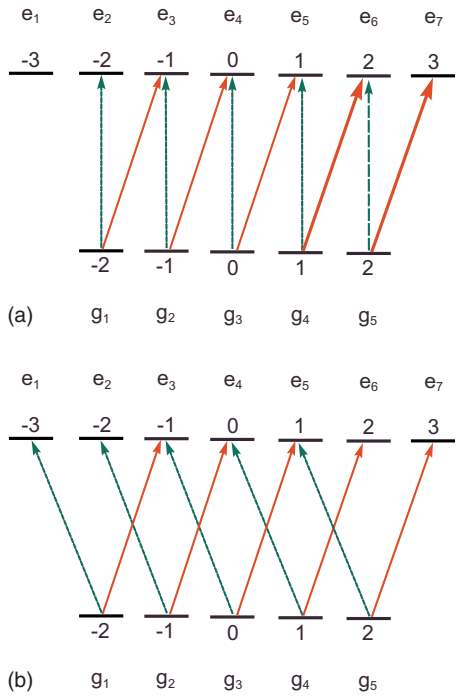

FIG. 1. (Color online) Energy-level scheme for $F_g=2\rightarrow F_e=3$ transition interacting with σ_+-polarized pump and (a) π-polarized and (b) σ_--polarized probe. The Zeeman sublevels are labeled by both the magnetic quantum numbers and g_j, $j=1-5$, for the ground state and e_i, $i=1-7$, for the excited state.

sition resembles that of the equivalent cycling transition when TOC is excluded from the calculation. In light of the importance of TOC in near-degenerate two-level systems that exhibit EIA, we explore its role in determining the pump and probe spectra discussed in this paper.

The probe and pump absorption spectra are analyzed by considering the contributions that derive from the individual $m_g\rightarrow m_e$ transitions. We then show how these contributions depend on the ground- and excited-state populations and Zeeman coherences, and investigate the role played by TOC. When the pump is σ_+ polarized and the probe π polarized, there is a tendency for the population to be swept toward the right of Fig. 1(a). When the pump general Rabi frequency Ω_1 exceeds the probe general Rabi frequency Ω_2, nearly all the population concentrates in the N-shaped system on the extreme right, so that the system can be modeled as an N system which is itself composed of a Λ and V system [3]. When the pump is weak, the probe spectrum is characterized by a sharp EIA peak at line center, and the pump spectrum also has an EIA peak that derives from the Λ system. However, the pump spectrum in the wings derives mainly from the V system, and is complementary to that of the probe spectrum. The sharp features in the spectra derive from the narrow ground-state Zeeman coherences, whose sign is inverted by TOC. When the pump is strong, however, the probe spectrum is split into four peaks, and the pump spectrum that derives mainly from the V system is completely complementary to it. In addition, the sharp features no longer appear, as the lifetimes of the ground Zeeman sublevels and the coherences between them are broadened by the strong coupling with the excited sublevels [11].

When $\Omega_1=\Omega_2$, all the individual transitions contribute to some extent to the absorption spectra. In the absence of TOC, all the inner transitions form a series of Λ systems characterized by electromagnetically induced transparency (EIT) [12] dips. However, the populations of the excited Zeeman sublevels, and the coherences between them, increase toward the right so that TOC turns the EIT dips into EIA peaks. The relative weights of the individual spectra determine whether the total spectrum has an EIA or EIT narrow feature. Generally, at low Rabi frequencies, both the pump and probe spectra have EIA peaks at line center and complementary behavior in the wings. At higher Rabi frequencies, the probe spectrum has an EIT dip and the pump spectrum, which is complementary to it, has an EIA peak within a broader EIT window.

For the case of a σ_+ pump and σ_- probe, the spectra have the same general shapes as for a σ_+ pump and π-polarized probe. When $\Omega_1>\Omega_2$, the main contributions to the spectrum come from the transitions toward the right, although the most extreme probe transition to the left may contribute when the pump is very weak. However, when $\Omega_1=\Omega_2$, the transitions to the left determine the probe spectrum whereas those to the right determine the pump spectrum.

II. THE BLOCH EQUATIONS

The system consists of one or more ground hyperfine states F_g and a single excited hyperfine state F_e interacting with a pump of frequency ω_1 and a probe of frequency ω_2. In order to write the equations in a compact manner, we label the Zeeman sublevels by g_j and e_i, where g_j is equivalent to $m_g=-F_g+(j-1)$ and e_i is equivalent to $m_e=-F_e+(i-1)$. We use the equations for the time evolution of the Zeeman sublevels as formulated by Renzoni [13], with the addition of decay from the ground and excited states to a reservoir [14], and collisions between the Zeeman sublevels of the ground states [15],

$$\dot{\rho}_{e_ie_j}=-(i\omega_{e_ie_j}+\Gamma)\rho_{e_ie_j}+(i/\hbar)\sum_{g_k}(\rho_{e_ig_k}V_{g_ke_j}-V_{e_ig_k}\rho_{g_ke_j})-\gamma(\rho_{e_ie_j}-\rho_{e_ie_i}^{eq})\delta_{e_ie_j}, \tag{1}$$

$$\dot{\rho}_{e_ig_j}=-(i\omega_{e_ig_j}+\Gamma'_{e_ig_j})\rho_{e_ig_j}+(i/\hbar)\left(\sum_{e_k}\rho_{e_ie_k}V_{e_kg_j}-\sum_{g_k}V_{e_ig_k}\rho_{g_kg_j}\right), \tag{2}$$

$$\dot{\rho}_{g_ig_i}=(i/\hbar)\sum_{e_k}(\rho_{g_ie_k}V_{e_kg_i}-V_{g_ie_k}\rho_{e_kg_i})+(\dot{\rho}_{g_ig_i})_{SE}-\gamma(\rho_{g_ig_i}-\rho_{g_ig_i}^{eq})+\sum_{g_k,k\neq i}\Gamma_{g_kg_i}\rho_{g_kg_k}-\Gamma_{g_i}\rho_{g_ig_i}, \tag{3}$$

$$\dot{\rho}_{g_ig_j}=-(i\omega_{g_ig_j}+\Gamma'_{g_ig_j})\rho_{g_ig_j}+(i/\hbar)\sum_{e_k}(\rho_{g_ie_k}V_{e_kg_j}-V_{g_ie_k}\rho_{e_kg_j})+(\dot{\rho}_{g_ig_j})_{SE} \tag{4}$$

where

$$(\dot{\rho}_{g_i g_j})_{\mathrm{SE}} = (2F_e+1)\Gamma_{F_e\to F_g}\sum_{q=-1,0,1}\sum_{m_e,m_e'=-F_e}^{F_e}(-1)^{-m_e-m_e'} \times\begin{pmatrix} F_g & 1 & F_e \\ -m_{g_i} & q & m_e\end{pmatrix}\rho_{m_e m_e'}\begin{pmatrix} F_e & 1 & F_g \\ -m_e' & q & m_{g_j}\end{pmatrix}, \quad (5)$$

with

$$\Gamma_{F_e\to F_g} = (2F_g+1)(2J_e+1)\begin{Bmatrix} F_e & 1 & F_g \\ J_g & I & J_e\end{Bmatrix}^2\Gamma \equiv b\Gamma. \quad (6)$$

In Eqs. (1)–(6), Γ is the *total* spontaneous emission rate from each $F_e m_e$ sublevel whereas $\Gamma_{F_e\to F_g}$ is the decay rate from F_e to one of the F_g states, Γ_{g_i} is the total collisional decay rate from sublevel g_i, $\Gamma_{g_i g_j}$ is the rate of transfer from sublevel $g_i\to g_j$, and γ is the rate of decay due to time of flight through the laser beams. The dephasing rates of the excited-to ground-state coherences are given by $\Gamma'_{e_i g_j}=\gamma+\frac{1}{2}(\Gamma+\Gamma_{g_j})+\Gamma^*$, where Γ^* is the rate of phase-changing collisions. The dephasing rates of the ground-state coherences are given by $\Gamma'_{g_i g_j}=\gamma+\frac{1}{2}(\Gamma_{g_i}+\Gamma_{g_j})+\Gamma^*_{g_i g_j}$, where $\Gamma^*_{g_i g_j}$ is the rate of phase-changing collisions. The frequency separation between levels a_i and b_j, including Zeeman splitting of the ground and excited levels due to an applied magnetic field, is given by $\omega_{a_i b_j}=(E_{a_i}-E_{b_j})/\hbar$, with $a,b=(g,e)$, and $\rho^{\mathrm{eq}}_{a_i a_i}$ with $a=(g,e)$ is the equilibrium population of state a_i, in the absence of any electrical fields. It should be noted that TOC derives from the last term in Eq. (4).

The interaction energy in the rotating-wave approximation for the transition from level g_j to e_i is written as

$$V_{e_i g_j} = -\mu_{e_i g_j}(E_1 e^{-i\omega_1 t}+E_2 e^{-i\omega_2 t}) \equiv -\hbar[V_{e_i g_j}(\omega_1)e^{-i\omega_1 t}+V_{e_i g_j}(\omega_2)e^{-i\omega_2 t}], \quad (7)$$

where $2V_{e_i g_j}(\omega_{1,2})$ are the pump and probe Rabi frequencies for the $F_e m_e\to F_g m_g$ transition, given by

$$2V_{e_i g_j}(\omega_{1,2}) = \frac{2\mu_{e_i g_j}E_{1,2}}{\hbar} = (-1)^{F_e-m_e}\begin{pmatrix} F_e & 1 & F_g \\ -m_e & q & m_g\end{pmatrix}\Omega_{1,2}, \quad (8)$$

where $\Omega_{1,2}=2\langle F_e\|\mu\|F_g\rangle E_{1,2}/\hbar$ are the general pump and probe Rabi frequencies for the $F_e\to F_g$ transition. In the absence of collisions, the width of the ground-state coherences is determined by $\gamma\ll\Gamma$. We will show here that, when the pump and probe Rabi frequencies $2V_{e_i g_j}(\omega_{1,2})<\Gamma$, these coherences give rise to sharp features in the absorption spectra. However, when $2V_{e_i g_j}(\omega_{1,2})>\Gamma$, the strong coupling between the ground and excited states tends to equalize the lifetimes of the states, so that ultranarrow features are no longer obtained [16].

When the probe is weak, the solution of those equations is performed in two stages. In the first, the pump interacts with the system, to all orders in its Rabi frequency. In the second stage, the interaction with the probe field E_2 is included to first order in the probe Rabi frequency so that $\rho_{e_i g_j}$ now oscillates at three frequencies: the pump frequency ω_1, the probe frequency ω_2, and the four-wave-mixing frequency $2\omega_1-\omega_2$, and the coherences and populations oscillate with frequencies $\pm(\omega_2-\omega_1)=\pm\delta$.

TABLE I. Frequencies of Fourier amplitudes

Pump	Probe	a_1	d	A	B
σ_+	π	$i-j$	1	$a_1(\omega_1-\omega_2)$	$a_{n-1}\omega_1-a_{n-2}\omega_2$
σ_-	π	$j-i$	−1	$a_1(\omega_1-\omega_2)$	$a_{n-1}\omega_1-a_n\omega_2$
σ_+	σ_-	$(j-i)/2$	−1/2	$a_1(\omega_2-\omega_1)$	$a_{n-2}\omega_2-a_n\omega_1$

When the probe is stronger, it is no longer possible to assume that the pump absorption and refraction are independent of the probe, so that the problem cannot be solved in two stages. When the pump or probe is σ polarized, and their Rabi frequencies are taken to all orders, each density-matrix element can oscillate at several frequencies. However, when they are π or $\sigma_\pm$ polarized, the problem is simplified since each density-matrix element oscillates at a single, individual frequency. These frequencies can be calculated using an algorithm that we have developed. In the steady state, the populations and coherences within the same hyperfine level can be written as

$$\rho_{a_i a_j} = \rho_{a_i a_j}(A)e^{-iAt} \quad (9)$$

with $a=(g,e)$, whereas the optical coherences $\rho_{e_i g_j}$ can be written as

$$\rho_{e_i g_j} = \rho_{e_i g_j}(B)e^{-iBt}. \quad (10)$$

In Eqs. (9) and (10), $\rho_{a_i a_j}(A)$ and $\rho_{e_i g_j}(B)$ are Fourier amplitudes at the frequencies $A(\omega_1,\omega_2)$ and $B(\omega_1,\omega_2)$. These frequencies can be expressed as terms in an arithmetic series, where the first term a_1 and the difference d are different for each combination of pump and probe polarizations. Their values are given in Table I for $F_e>F_g$, $F_e=F_g$, and $F_e<F_g$ transitions (labeled $n=1,2,3$, respectively). When the pump and probe polarizations are interchanged, the pump and probe frequencies are also interchanged.

In this paper, we discuss the steady-state pump and probe absorption $\alpha(\omega_{1,2})$, which are given by [17]

$$\alpha(\omega_{1,2}) = \frac{4\pi\omega_0 N}{\hbar c}\sum_{e_i g_j}\frac{|\mu_{e_i g_j}|^2}{V_{e_i g_j}(\omega_{1,2})}\mathrm{Im}[\rho_{e_i g_j}(\omega_{1,2})], \quad (11)$$

where N is the density of atoms and ω_0 is the frequency of the ground to excited state transition in the absence of the magnetic field.

Using Eqs. (1)–(4), (7), (10), and (11), we write the contribution of each optical coherence to $\alpha(\omega_{1,2})$ for the case where the pump is σ_+ polarized and the probe π polarized:

$$\rho_{e_i g_j}(\omega_1) = [\eta_{e_i g_j}(\omega_1)-i\kappa_{e_i g_j}(\omega_1)][(\rho_{e_i e_i}-\rho_{g_j g_j})V_{e_i g_j}(\omega_1) + \rho_{e_i e_{i-1}}(\omega_1-\omega_2)V_{e_{i-1} g_j}(\omega_2) - \rho_{g_{j+1} g_j}(\omega_1-\omega_2)V_{e_i g_{j+1}}(\omega_2)], \quad (12)$$

$$\rho_{e_i g_j}(\omega_2) = [\eta_{e_i g_j}(\omega_2) - i\kappa_{e_i g_j}(\omega_2)][(\rho_{e_i e_i} - \rho_{g_j g_j})V_{e_i g_j}(\omega_2) + \rho_{e_i e_{i+1}}(\omega_2 - \omega_1)V_{e_{i+1} g_j}(\omega_1) - \rho_{g_{j-1} g_j}(\omega_2 - \omega_1)V_{e_i g_{j-1}}(\omega_1)], \quad (13)$$

where

$$\eta_{e_i g_j}(\omega_{1,2}) = \frac{\Delta_{e_i g_j}(\omega_{1,2})}{\Gamma'^2_{e_i g_j} + \Delta^2_{e_i g_j}(\omega_{1,2})} \quad (14)$$

and

$$\kappa_{e_i g_j}(\omega_{1,2}) = \frac{\Gamma'_{e_i g_j}}{\Gamma'^2_{e_i g_j} + \Delta^2_{e_i g_j}(\omega_{1,2})} \quad (15)$$

with

$$\Delta_{e_i g_j}(\omega_{1,2}) = \omega_{e_i g_j} - \omega_{1,2}. \quad (16)$$

From Eqs. (12) and (13), we see that the only Zeeman coherences that contribute directly to the optical coherences are those between nearest-neighboring ground or excited Zeeman sublevels at frequencies $\pm\delta$. However, as can be seen from Eqs. (1)–(4), these Zeeman coherences are themselves determined by the optical coherences at the four-wave-mixing frequencies $\pm(2\omega_2-\omega_1)$ and $\pm(2\omega_1-\omega_2)$ which, in turn, are determined by Zeeman coherences between the next-nearest-neighboring sublevels at the frequencies $\pm 2\delta$, and so on. The highest frequency at which the Zeeman coherences oscillate is given by $\pm a_{1_{\max}}\delta$ where $a_{1_{\max}}$ is the maximum value of a_1 which is defined in Table I: for a σ_+-polarized pump and a π-polarized probe, $a_{1_{\max}}=F_g+F_e$ for all types of $F_g \rightarrow F_e$ transitions.

For the case where the pump is σ_+ polarized and the probe σ_- polarized, the contribution of each optical coherence to $\alpha(\omega_{1,2})$ can be written as

$$\rho_{e_i g_j}(\omega_1) = [\eta_{e_i g_j}(\omega_1) - i\kappa_{e_i g_j}(\omega_1)][(\rho_{e_i e_i} - \rho_{g_j g_j})V_{e_i g_j}(\omega_1) + \rho_{e_i e_{i-2}}(\omega_1 - \omega_2)V_{e_{i-2} g_j}(\omega_2) - \rho_{g_{j+2} g_j}(\omega_1 - \omega_2)V_{e_i g_{j+2}}(\omega_2)], \quad (17)$$

$$\rho_{e_i g_j}(\omega_2) = [\eta_{e_i g_j}(\omega_2) - i\kappa_{e_i g_j}(\omega_2)][(\rho_{e_i e_i} - \rho_{g_j g_j})V_{e_i g_j}(\omega_2) + \rho_{e_i e_{i+2}}(\omega_2 - \omega_1)V_{e_{i+2} g_j}(\omega_1) - \rho_{g_{j-2} g_j}(\omega_2 - \omega_1)V_{e_i g_{j-2}}(\omega_1)]. \quad (18)$$

In this case, the Zeeman coherences that contribute directly to the optical coherences are those between *next*-nearest neighbors at frequencies $\pm\delta$. However, as before, these Zeeman coherences are themselves determined by higher-order Zeeman coherences. For this case, $a_{1_{\max}}=F_>$, where $F_>$ is the larger of F_g and F_e.

III. RESULTS AND DISCUSSION

A. $F_g \rightarrow F_e=F_g+1$ transition interacting with σ_+-polarized pump and π-polarized probe

The spectra are calculated for the $F_g=2 \rightarrow F_e=3$ transition in the D_2 line of ^{87}Rb interacting with a σ_+-polarized pump and π-polarized probe; the energy-level scheme is shown schematically in Fig. 1(a). We assume throughout that the pump is on resonance so that $\Delta_{e_i g_j}(\omega_1)=0$, and that $\gamma/\Gamma=0.001$. The absorption is always given in units of cm^{-1}. It can be seen from Eqs. (11)–(13), that the contribution to the total probe absorption from the $g_i \rightarrow e_{i+1}$, $i=2-5$, transition is determined by the two-photon coherence $\rho_{g_{i-1} g_i}(\omega_2-\omega_1)$ whereas the contribution to the $g_{i-1} \rightarrow e_{i+1}$, $i=2-5$, pump absorption spectrum is determined by $\rho_{g_i g_{i-1}}(\omega_1-\omega_2)=\rho^*_{g_{i-1} g_i}(\omega_2-\omega_1)$. Thus, for those cases where the contribution of the ground-state population and the real part of the ground-state coherence determine the absorption, it would seem reasonable to suppose that the inner probe and pump transitions in Fig. 1(a) form a series of Λ systems, characterized by EIT dips at line center, in both the pump and probe spectra. However, this is true only when TOC is neglected. Both the ground- and excited-state populations are swept toward the right for these pump and probe polarizations, so that the excited-state coherence, although small, also increases toward the right. The effect of TOC from the excited state to the ground state is either to reduce the negative value of the real part of the coherence, or to turn it from negative to positive, leading to EIA peaks. This explains the tendency to obtain EIT peaks for the inner transitions to the left of Fig. 1(a) and EIA peaks for the inner transitions toward the right.

1. $\Omega_1 > \Omega_2$; $\Omega_1 < \Gamma$

We first discuss the case where the general Rabi frequency of the σ_+-polarized pump Ω_1 is greater than that of the π-polarized probe Ω_2, but the probe is still sufficiently strong to affect the pump absorption spectrum. For simplicity, we consider the case where $\Omega_1, \Omega_2 < \Gamma$. The probe absorption spectrum for $\Omega_1/\Gamma=0.5$ and $\Omega_2/\Gamma=0.1$ as a function of δ/Γ is shown in Fig. 2(a). It is characterized by a sharp EIA peak centered at $\delta/\Gamma=0$ and is similar to the spectrum obtained for a very weak probe [3]. When the contributions to the absorption that derive from the various transitions are analyzed using Eq. (11), it is found that the main contribution to the probe absorption comes from the term proportional to $\mathrm{Im}[\rho_{e_6 g_5}(\omega_2)]$, shown in Fig. 2(b), with a smaller contribution of similar shape from the term proportional to $\mathrm{Im}[\rho_{e_5 g_4}(\omega_2)]$ (not shown). This suggests that, as for the case of a very weak probe, the population is swept toward the right so that the transition can be modeled, to a reasonable approximation, as an N-shaped system composed of Zeeman sublevels $g_{4,5}$ and $e_{6,7}$, as shown in Fig. 1(a). The pump absorption spectrum, shown in Fig. 3(a), like that of the probe [Fig. 2(a)], is characterized by an EIA peak at line center. However, the spectrum in the wings is a mirror image of that of the probe, that is, the pump absorption decreases when the probe spectrum increases. The main contributions to the pump spectrum come from the terms in Eq. (11) proportional to $\mathrm{Im}[\rho_{e_6 g_4}(\omega_1)]$ and $\mathrm{Im}[\rho_{e_7 g_5}(\omega_1)]$, shown in Figs. 3(b) and 3(c), that is, from the two transitions of the N system that interact with the pump. At line center, the main contribution comes from the $g_4 \rightarrow e_6$ transition, whereas in the wings the $g_5 \rightarrow e_7$ transition dominates. The probe and pump spectra shown in Figs. 2 and 3 resemble those calcu-

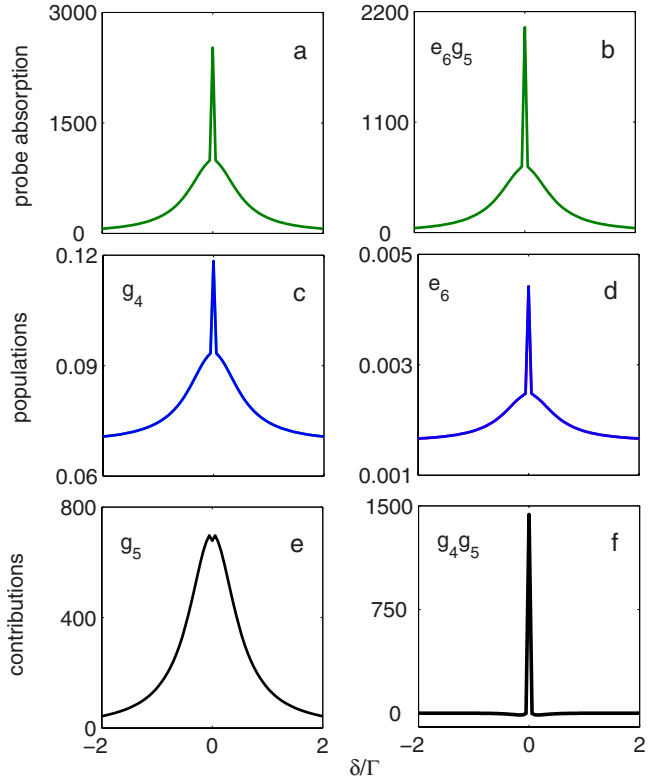

FIG. 2. (Color online) Probe absorption spectrum in presence of TOC as a function of δ/Γ for interaction of an $F_g=2\rightarrow F_e=3$ transition with σ_+-polarized pump and π-polarized probe lasers: (a) total probe absorption; (b) main contribution to total probe absorption spectrum from $g_5\rightarrow e_6$ transition; (c) spectrum of population in sublevel g_4; (d) spectrum of population in sublevel e_6; (e) contribution to spectrum in (b) from population in g_5; (f) contribution to spectrum in (b) from real part of g_4g_5 coherence. $\Omega_1/\Gamma=0.5$, $\Omega_1/\Gamma=0.1$, and $\gamma/\Gamma=0.001$. The absorption and its contributions are in units of cm^{-1}.

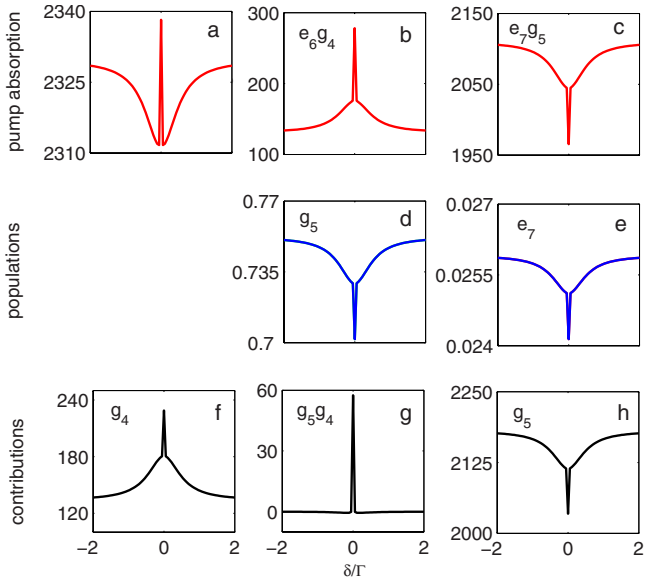

FIG. 3. (Color online) Pump absorption spectrum in presence of TOC as a function of δ/Γ for interaction of an $F_g=2\rightarrow F_e=3$ transition with σ_+-polarized pump and π-polarized probe lasers: (a) total pump absorption; (b) main contribution to total pump absorption spectrum from $g_4\rightarrow e_6$ transition; (c) main contribution to total pump absorption spectrum from $g_5\rightarrow e_7$ transition, (d) spectrum of population in sublevel g_5; (e) spectrum of population in sublevel e_7; (f) contribution to spectrum in (b) from population in g_4; (g) contribution to spectrum in (b) from real part of g_5g_4 coherence; (h) contribution to spectrum in (c) from population in g_5. Parameters and units as in Fig. 2.

lated for a pure N-shaped system, as shown in Fig. 6 of [3]. We will see below that, for higher pump and probe Rabi frequencies, the pump and probe spectra are complete mirror images of each other, as was shown in Fig. 7 of [3] for a pure N-shaped system.

As discussed in [3], the N-shaped system itself is composed of a V-shaped system (g_5 and $e_{6,7}$) and a Λ-shaped system ($g_{4,5}$ and e_6). The pump transition $g_5\rightarrow e_7$ is part of a V system whereas the $g_4\rightarrow e_6$ transition is part of a Λ system. We can see from Figs. 2(c) and 2(d) that the spectra of the populations in the sublevels g_4 and e_6 resemble the contributions to the probe absorption spectrum and to the pump spectrum, shown in Figs. 2(b) and 3(b), whereas the contribution to the pump spectrum, shown in Fig. 3(c), resembles the population spectra in g_5 (the most populated sublevel) and e_7, shown in Figs. 3(d) and 3(e). Let us first consider the V system, where both transitions share the same ground state g_5. When the absorption of the probe interacting with the $g_5\rightarrow e_6$ transition increases, the population in the Zeeman sublevel g_5 decreases. Thus, the spectrum of the population in g_5, shown in Fig. 3(d), is the mirror image of the probe absorption spectrum, shown in Fig. 2(b). The pump absorption on the $g_5\rightarrow e_7$ transition, shown in Fig. 3(c), simply reflects the ground-state population spectrum, as does the population in the excited sublevel e_7, shown in Fig. 3(e). By contrast, in the Λ system, the transitions induced by the probe and pump share the same excited state e_6. As a result, the probe and pump absorption spectra have the same shape [compare Figs. 2(b) and 3(b)]. The pump spectrum for the $g_4\rightarrow e_6$ transition, shown in Fig. 3(b), reflects the spectra of the g_4 and e_6 populations, shown in Figs. 2(c) and 2(d). These populations increase when the probe absorption increases, and vice versa, as a result of optical pumping induced by the probe.

The probe EIA spectrum obtained for $F_g\rightarrow F_e=F_g+1$ atomic transitions interacting with perpendicularly polarized pump and probe fields has been attributed to TOC from the excited to the ground state [6,7]. Using Eqs. (11) and (13), we plot in Figs. 2(e) and 2(f) the main contributions to the probe absorption that derives from the $g_5\rightarrow e_6$ transition, shown in Fig. 2(b). In Fig. 2(e), we plot the contribution proportional to $\rho_{g_5g_5}$ and in Fig. 2(f) that proportional to $\mathrm{Re}[\rho_{g_4g_5}(\omega_2-\omega_1)]$; the terms proportional to the excited-state population $\rho_{e_6e_6}$, the two-photon excited-state Zeeman coherence $\rho_{e_6e_7}(\omega_2-\omega_1)$, and $\mathrm{Im}[\rho_{g_4g_5}(\omega_2-\omega_1)]$ give very small contributions. It is obvious that the EIA peak derives from the sharp, positive peak in the two-photon ground-state Zeeman coherence. Similarly, using Eqs. (11) and (12), we plot the main contributions to the pump absorption that derives

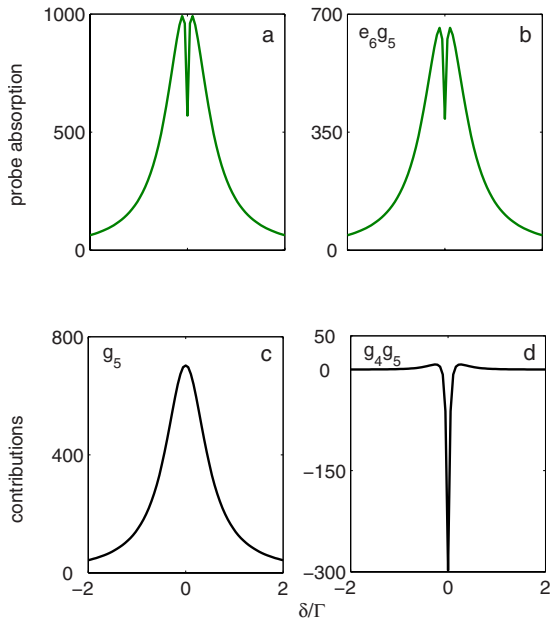

FIG. 4. (Color online) Probe absorption spectrum in absence of TOC as a function of δ/Γ for interaction of an $F_g=2\rightarrow F_e=3$ transition with σ_+-polarized pump and π-polarized probe lasers: (a) total probe absorption; (b) main contribution to total probe absorption spectrum from $g_5\rightarrow e_6$ transition; (e) contribution to spectrum in (b) from population in g_5; (f) contribution to spectrum in (b) from real part of g_4g_5 coherence. Parameters and units as in Fig. 2.

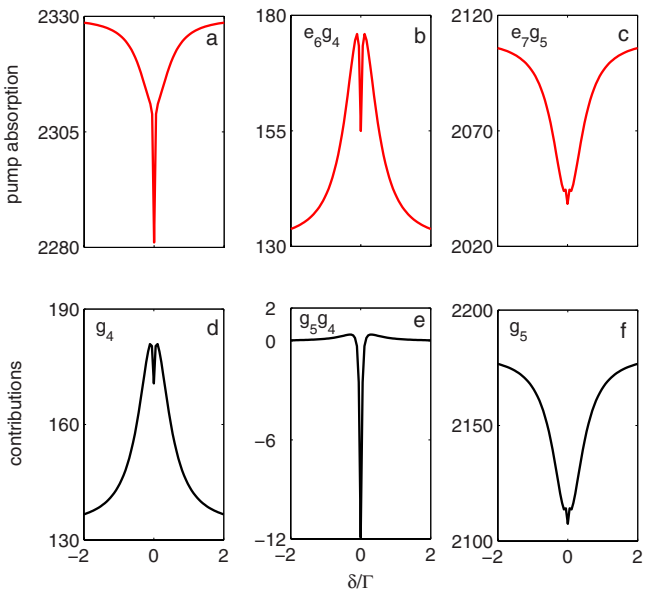

FIG. 5. (Color online) Pump absorption spectrum in absence of TOC as a function of δ/Γ for interaction of an $F_g=2\rightarrow F_e=3$ transition with σ_+-polarized pump and π-polarized probe lasers: (a) total pump absorption; (b) main contribution to total pump absorption spectrum from $g_4\rightarrow e_6$ transition; (c) main contribution to total pump absorption spectrum from $g_5\rightarrow e_7$ transition; (d) contribution to spectrum in (b) from population in g_4; (e) contribution to spectrum in (b) from real part of g_5g_4 coherence; (f) contribution to spectrum in (c) from population in g_5. Parameters and units as in Fig. 2.

from the $g_4\rightarrow e_6$ transition [see Fig. 3(b)], in Figs. 3(f) and 3(g). The sharp feature at line center appears in the component that derives from the population in g_4 and is reinforced by the contribution of the ground-state Zeeman coherence $\mathrm{Re}[\rho_{g_5g_4}(\omega_2-\omega_1)]$. In Fig. 3(h), we plot the main contribution to the pump absorption that derives from the $g_5\rightarrow e_7$ transition, shown in Fig. 3(c). In this case, only the contribution proportional to the g_5 population gives a significant contribution; there is no contribution from the ground-state coherence and only a small contribution from the excited-state coherence.

In order to investigate the role of TOC, we plot the total probe and pump absorption spectra in the absence of TOC, in Figs. 4(a) and 5(a), the main contribution to the probe spectrum in Figs. 4(b), and the main contributions to the pump spectrum in Figs. 5(b) and 5(c). The correlation between these contributions and the population spectra are the same as in the presence of TOC and are not repeated here. However, the contributions of the ground-state Zeeman coherence $\rho_{g_4g_5}$ to the probe and pump spectra are very significant. We see from Fig. 4(d) that the two-photon coherence $\mathrm{Re}[\rho_{g_4g_5}(\omega_2-\omega_1)]$ now gives a sharp, negative contribution to the probe absorption, leading to a dip in the probe absorption at line center. Indeed, our calculations show that all the $\rho_{g_{j-1}g_j}$, $j=2-5$, coherences give sharp negative contributions to the individual probe transitions, and thus to the total absorption. Similarly, it can be seen from Fig. 5(e) that $\mathrm{Re}[\rho_{g_5g_4}(\omega_2-\omega_1)]$ contributes a sharp dip to the pump absorption from the $g_4\rightarrow e_6$ transition, shown in Fig. 5(b). This gives a dip at line center in the total pump absorption [Fig. 5(a)] whereas the behavior in the wings derives from the pump absorption in the $g_5\rightarrow e_7$ transition which derives mainly from the population in g_5 [Fig. 5(f)] with a small contribution from the population in e_7. Thus one can say that the effect of TOC in this case is to turn the contribution of the ground-state coherence from negative to positive.

2. $\Omega_1=\Omega_2<\Gamma$

We now turn to the case of equal general Rabi frequencies where $\Omega_1=\Omega_2<\Gamma$. The essential difference between this case and the previous one is that the system no longer resembles an N-shaped system, as the population is spread out over all the ground-state Zeeman sublevels. In Figs. 6(a) and 7(a), we plot the probe absorption spectrum in the presence and absence of TOC. It is characterized by a sharp EIA peak at line center, in the presence of TOC, and a dip, in the absence of TOC. The spectra, in the presence and absence of TOC, are similar to those for the case where $\Omega_1/\Gamma=0.5$ and $\Omega_2/\Gamma=0.1$, shown in Figs. 2(a) and 4(a). The contributions to the total probe absorption from the various $g_i\rightarrow e_{i+1}$, $i=1-5$, transitions, calculated from Eqs. (11) and (13), are shown in Figs. 6(b)–6(f), in the presence of TOC, and in Figs. 7(b)–7(f), in the absence of TOC. We see that all the probe transitions contribute significantly to the total absorption. The reason for this is obvious from inspection of Figs. 6(g)–6(k) and Figs. 7(g)–7(k), where we plot the contribution of the population in the g_i sublevels to the probe absorption in the $g_i\rightarrow e_{i+1}$ transitions, in the presence and absence

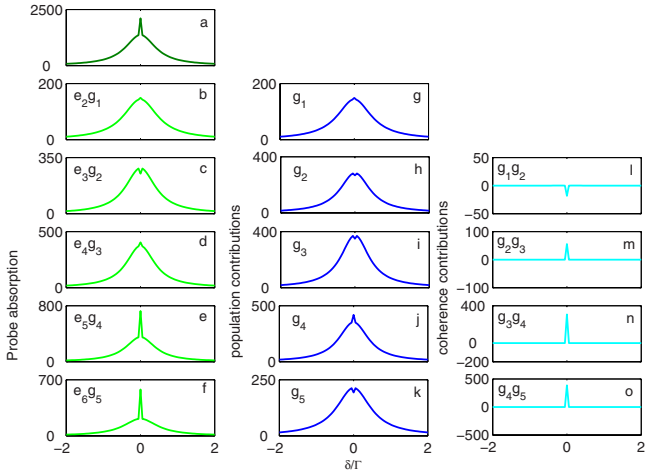

FIG. 6. (Color online) Probe absorption spectrum in presence of TOC as a function of δ/Γ for interaction of an $F_g=2\rightarrow F_e=3$ transition with σ_+-polarized pump and π-polarized probe lasers: (a) total probe absorption; (b)–(f) contributions to total probe absorption spectrum from $g_i\rightarrow e_{i+1}$, $i=1-5$, transitions; (g)–(k) contribution of population in sublevels g_i, $i=1-5$, to spectra in (b)–(f); (l)–(o) contributions of real part of Zeeman coherence $g_{i-1}g_i$, $i=2-5$, to spectra in (b)–(f). $\Omega_1/\Gamma=0.1$, $\Omega_2/\Gamma=0.1$, and $\gamma/\Gamma=0.001$. The absorption and its contributions are in units of cm^{-1}.

of TOC. We see that the population is distributed over all the g_i sublevels, and that the population contributions have either a small narrow peak or dip at line center. The contributions to the individual probe absorptions $g_i\rightarrow e_{i+1}$, $i=2-5$, from the real parts of the $g_{i-1}g_i$ two-photon Zeeman coherences are shown in Figs. 6(l)–6(o), in the presence of TOC, and in Figs. 7(l)–7(o), in the absence of TOC. We see that, in the absence of TOC, all the two-photon coherences give a sharp negative contribution near line center. When TOC is included, the contributions become either less negative [Fig. 6(l)] or positive [Fig. 6(m)–6(o)], leading to EIA peaks in the individual and total probe absorptions.

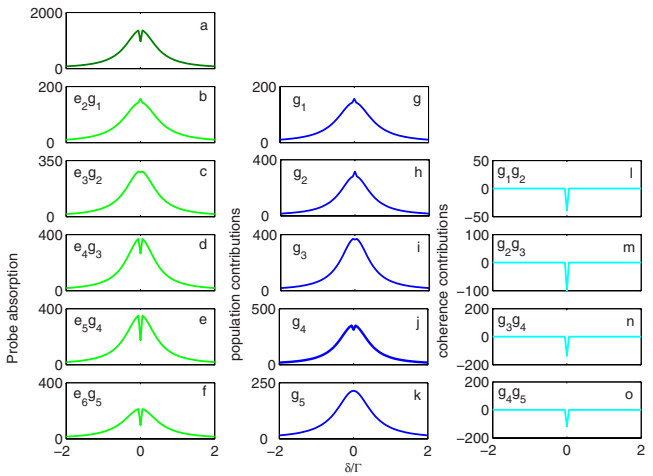

FIG. 7. (Color online) Probe absorption spectrum in absence of TOC as a function of δ/Γ for interaction of an $F_g=2\rightarrow F_e=3$ transition with σ_+-polarized pump and π-polarized probe lasers: (a) total probe absorption; (b)–(f) contributions to total probe absorption spectrum from $g_i\rightarrow e_{i+1}$, $i=1-5$, transitions; (g)–(k) contribution of population in sublevels g_i, $i=1-5$, to spectra in (b)–(f); (l)–(o) contribution of real part of Zeeman coherence $g_{i-1}g_i$, $i=2-5$, to spectra in (b)–(f). Parameters and units as in Fig. 6.

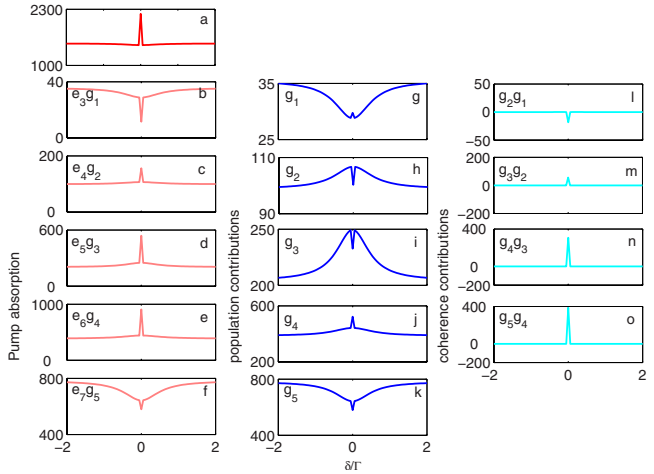

FIG. 8. (Color online) Pump absorption spectrum in presence of TOC as a function of δ/Γ for interaction of an $F_g=2\rightarrow F_e=3$ transition with σ_+-polarized pump and π-polarized probe lasers: (a) total pump absorption; (b)–(f) contributions to total pump absorption spectrum from $g_i\rightarrow e_{i+2}$, $i=1-5$, transitions; (g)–(k) contribution of population in sublevels g_i, $i=1-5$, to spectra in (b)–(f); (l)–(o) contribution of Zeeman coherence $g_{i+1}g_i$, $i=1-4$, to spectra in (b)–(f). Parameters and units as in Fig. 6.

In Figs. 8(a) and 9(a), we plot the pump absorption spectrum with and without TOC. The pump spectrum, like the probe absorption spectrum, is characterized by a sharp EIA

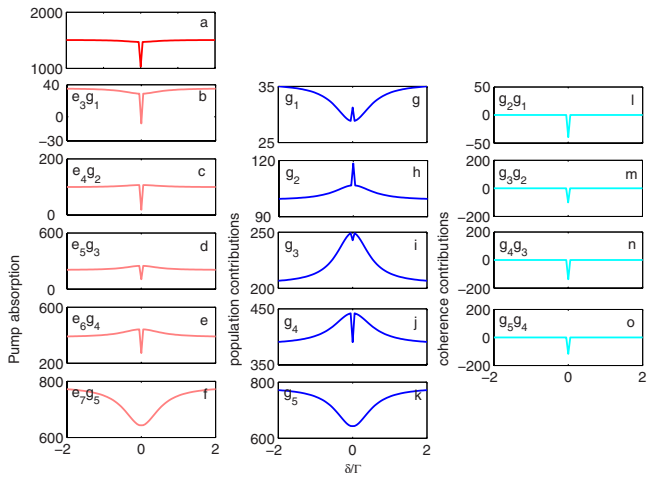

FIG. 9. (Color online) Pump absorption spectrum in absence of TOC as a function of δ/Γ for interaction of a $F_g=2\rightarrow F_e=3$ transition with σ_+-polarized pump and π-polarized probe lasers: (a) total pump absorption; (b)–(f) contributions to total pump absorption spectrum from $g_i\rightarrow e_{i+2}$, $i=1-5$, transitions; (g)–(k) contribution of population in sublevels g_i, $i=1-5$, to spectra in (b)–(f); (l)–(o) contribution of Zeeman coherence $g_{i+1}g_i$, $i=1-4$, to spectra in (b)–(f). Parameters and units as in Fig. 6.

peak at line center, in the presence of TOC, and a dip, in the absence of TOC. In both the presence and absence of TOC, the behavior in the wings is the opposite of that exhibited by the probe. The contributions to the total pump absorption from the various $g_i \rightarrow e_{i+2}$, $i=1-5$ transitions are shown in Figs. 8(b)–8(f), in the presence of TOC, and in Figs. 9(b)–9(f), in its absence. Most of the transitions are characterized by an EIA peak in the presence of TOC and a dip in its absence. The highest contribution to the absorption comes from the $g_5 \rightarrow e_7$ transition in the wings, and the $g_4 \rightarrow e_6$ transition at line center. However, all the transitions make a significant contribution. The contributions to the individual pump absorptions $g_i \rightarrow e_{i+2}$, $i=1-5$, from the populations in the g_i sublevels are plotted in Figs. 8(g)–8(k) and Figs. 9(g)–9(k), and those from the real parts of the $g_{i+1}g_i$, $i=1-4$, two-photon Zeeman coherences are shown in Figs. 8(l)–8(o) and Figs. 9(l)–9(o). It can be seen from Eqs. (11)–(13) and Figs. 6(l)–6(o), and Figs. 8(l)–8(o), that, near line center, the contributions of the coherences to the $g_i \rightarrow e_{i+2}$ pump spectra are equal to their contributions to the probe $g_{i+1} \rightarrow e_{i+2}$ spectra, due to the equality of the general pump and probe Rabi frequencies. The correlation between the pump and probe absorption spectra for the individual transitions and the populations in the Zeeman sublevels, discussed in Sec. III A 1 for the case where most of the population is swept into an N system [see Fig. 1(a)], holds in the present case for the same N system and also for the V system formed by the sublevels g_1, e_2, and e_3.

3. $\Omega_1 > \Omega_2$; $\Omega_1 > \Gamma$

In both the cases discussed so far, the sharp features at line center were in the same direction whereas, in the wings, the spectra were mirror images of each other. We now discuss a case where the pump and probe spectra are mirror images of each other, both at line center and in the wings. In Fig. 10(a), we plot the probe absorption spectrum in the presence and absence of TOC, for the case where $\Omega_1/\Gamma=10$ and $\Omega_2/\Gamma=0.6$. In the presence of TOC, the spectrum splits into four well-resolved peaks, whereas in the absence of TOC, the two central peaks overlap. The spectra have the same shape as in the case of a strong pump and a very weak probe [3,18], and are also similar to the spectra obtained for an intense pump and weak probe interacting with a pure N system [18], where the positions of the peaks can be calculated using dressed states [3]. The major contribution to the probe spectrum comes from the $g_5 \rightarrow e_6$ transition, shown in Fig. 10(b). The pump absorption spectrum, shown in Fig. 11(a) is the mirror image of the probe spectrum, and as can be seen from Fig. 11(b), has the same general shape as the contribution from the $g_5 \rightarrow e_7$ transition. However, in order to reproduce the total pump absorption, the small contribution from the $g_4 \rightarrow e_6$ transition, which is the mirror image of that from the $g_5 \rightarrow e_7$ transition, must also be included. As in the case discussed in Sec. I, there is a strong correlation between the major contributions to the probe and pump absorption spectra and the populations in the ground and excited Zeeman sublevels: the population spectra of g_4 and e_6, shown in Figs. 10(c) and 10(d), resemble the probe absorption spectrum, whereas the population spectra of g_5 and e_7, shown in Figs.

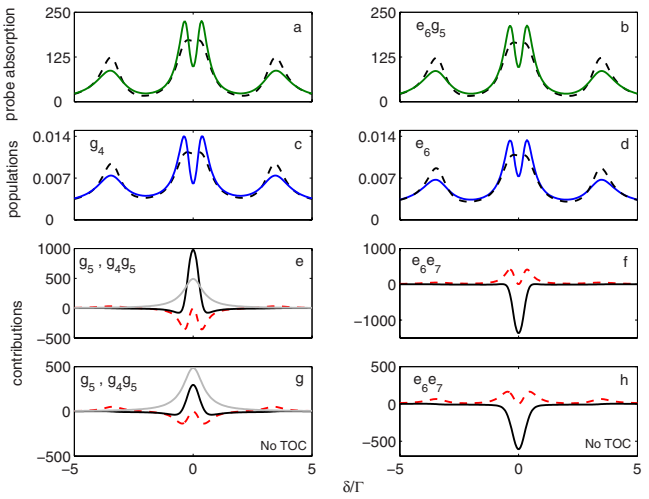

FIG. 10. (Color online) Probe absorption spectrum as a function of δ/Γ for interaction of an $F_g=2 \rightarrow F_e=3$ transition with σ_+-polarized pump and π-polarized probe lasers: (a) total probe absorption; (b) contribution to total probe absorption spectrum from $g_5 \rightarrow e_6$ transition; (c) population in sublevel g_4; (d) population in sublevel e_6; (e) contributions to (b) from population in g_4 (gray solid line), and real (black solid line) and imaginary (dashed line) parts of g_4g_5 coherence; (f) contributions to (b) from real (solid line) and imaginary (dashed line) parts of e_6e_7 coherence; (g) same as (e) but without TOC; (h) same as (f) but without TOC. In (a)–(d), solid line is with TOC, dashed line is without TOC. $\Omega_1/\Gamma=10$, $\Omega_2/\Gamma=0.6$, and $\gamma/\Gamma=0.001$. The absorption and its contributions are in units of cm^{-1}.

11(c) and 11(d), resemble the pump absorption spectrum. From an inspection of the populations, we see that nearly all the population is shared between g_5 and e_7. This fact, taken together with the mirror image behavior of the pump and probe spectra, suggests that in this case the atomic transition

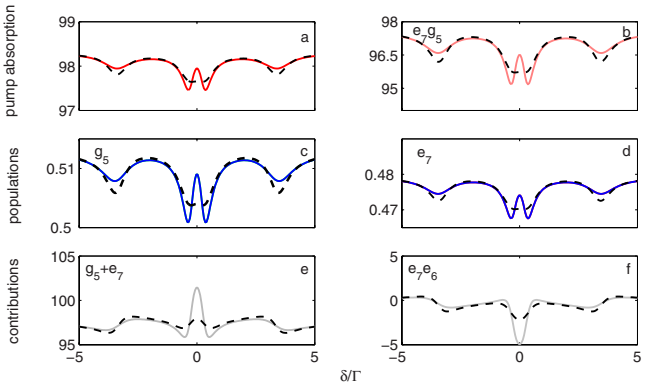

FIG. 11. (Color online) Pump absorption spectrum as a function of δ/Γ for interaction of an $F_g=2 \rightarrow F_e=3$ transition in D_2 line of ^{87}Rb with σ_+-polarized pump and π-polarized probe lasers: (a) total pump absorption; (b) contribution to total pump absorption spectrum from $g_5 \rightarrow e_7$ transition; (c) population in sublevel g_5; (d) population in sublevel e_7; (e) sum of contributions to spectrum in (b) from populations in g_5 and e_7; (f) contributions to spectrum in (b) from real part of e_7e_6 coherence. Solid lines are with TOC and dashed lines are without TOC. Parameters and units as in Fig. 10.

can be modeled as an N-shaped system, with the major contribution coming from the V-shaped system composed of sublevels g_5, e_6, and e_7 [3].

The main contributions to the $g_5 \rightarrow e_6$ probe absorption, calculated from Eqs. (11) and (13), are shown in Figs. 10(e) and 10(f) (with TOC) and in Figs. 10(g) and 10(h) (without TOC). In Figs. 10(e) and 10(g), we show the contribution from the population in g_5 and from the real and imaginary parts of the $g_4 g_5$ coherence, and in Figs. 10(f) and 10(h), we show the contributions from the real and imaginary parts of the $e_6 e_7$ coherence. We see from these figures that the contributions from the imaginary parts of the ground- and excited-state coherences give the main contribution to the outer two peaks in the probe absorption, and determine the positions of the two inner peaks. In contrast to the case discussed in Sec. I and shown in Figs. 2(f) and 4(d), where TOC inverted the coherence contribution, here the general shape of the coherences is unchanged by the inclusion of TOC. However, the central features in both the ground- and excited-state coherences are narrower and more intense in the presence of TOC than in its absence, whereas the population is identical in both cases. This is the reason that the two inner peaks are clearly resolved in the presence of TOC but not in its absence. The main contributions to the $g_5 \rightarrow e_7$ pump absorption, calculated from Eqs. (11) and (12), with and without TOC, are shown in Figs. 11(e) and 11(f). We see that the central feature in the sum of the contributions from the g_5 and e_7 populations, shown in Fig. 11(e), and also in the real part of the excited-state coherence contribution, shown in Fig. 11(f), are narrower and more intense when TOC is included. Again this leads to the inner dips being clearly resolved in the presence of TOC but not in its absence. In this case, the ultranarrow features in the populations, coherences, and absorption spectra, obtained for the case where $\Omega_{1,2} < \Gamma$ do not occur. This is due to the strong coupling between the ground- and excited-states which has the effect of equalizing their lifetimes [16]. An explicit expression for the effective value of γ for a Λ system interacting with strong fields is given in Eq. (11) of [11].

4. $\Omega_1 = \Omega_2 > \Gamma$

When both the pump and probe are strong and equally intense, all the transitions contribute to some extent to the probe and pump spectra. Generally, in the presence of TOC, the probe transitions to the left in Fig. 1(a) have dips at line center whereas those to the right have peaks. Depending on the relative values of the contributions, the total absorption can be characterized by either a peak or a dip. For example, when $\Omega_1/\Gamma = \Omega_2/\Gamma = 2$, the probe spectrum has an EIA peak at line center [see Fig. 12(a)] whereas when $\Omega_1/\Gamma = \Omega_2/\Gamma = 6$, it has a dip [see Fig. 12(b)]. It should be noted that $\Omega_{1,2} > \Gamma$ does not necessarily imply that $2V_{e_i g_j}(\omega_{1,2}) > \Gamma$ for all the individual pump and probe transitions. Thus although the peak and dip are not as narrow as in the case where $\Omega_{1,2} < \Gamma$, they are still quite narrow. In both cases, the pump spectrum in the wings is mostly determined by the contribution from the $g_5 \rightarrow e_7$ transition since the g_5 sublevel is the most populated sublevel when the probe is detuned, and its population increases with increasing detuning. However, at line center, the $g_4 \rightarrow e_6$ spectrum which has a peak gives the main contribution. These effects, taken together, produce a pump spectrum characterized by a narrow peak at line center inside a dip [see Figs. 12(c) and 12(d)]. This is very similar to the situation shown in Figs. 3 and 8. Thus, once again, we find that the pump spectrum is complementary to the probe spectrum in the wings, and may have the same or opposite behavior at line center. For this case, unlike the case of weak, equal pump and probe Rabi frequencies, presented in Sec. III A 2, all the terms in Eqs. (12) and (13) contribute to the individual probe and pump absorptions, and so a simple interpretation is no longer possible.

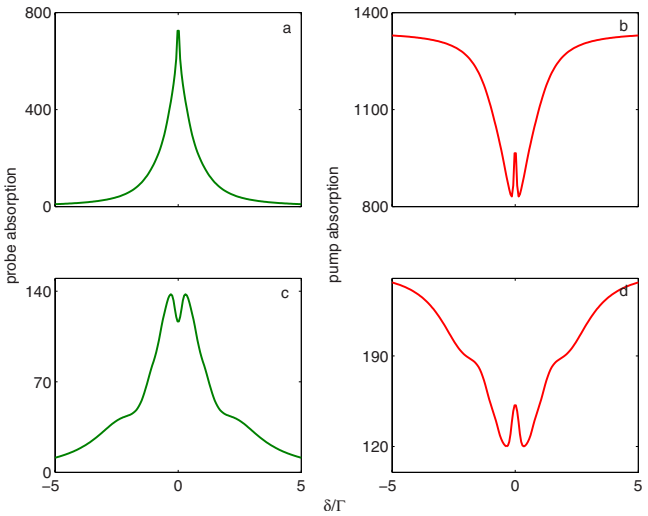

FIG. 12. (Color online) Probe and pump absorption spectrum as a function of δ/Γ for interaction of an $F_g = 2 \rightarrow F_e = 3$ transition in D_2 line of ^{87}Rb with σ_+-polarized pump and π-polarized probe lasers: (a) total probe absorption for $\Omega_1/\Gamma = \Omega_2/\Gamma = 2$; (b) total pump absorption for $\Omega_1/\Gamma = \Omega_2/\Gamma = 2$; (c) total probe absorption for $\Omega_1/\Gamma = \Omega_2/\Gamma = 6$; (d) total pump absorption for $\Omega_1/\Gamma = \Omega_2/\Gamma = 6$. $\gamma/\Gamma = 0.001$ and the absorption and its contributions are in units of cm^{-1}.

B. $F_g \rightarrow F_e = F_g + 1$ transition interacting with σ_+-polarized pump and σ_--polarized probe

We now turn to the case of a σ_+ pump and a σ_- probe, shown in Fig. 1(b). In Fig. 13(a), 13(c), and 13(e), we plot the probe spectra for the same pump and probe Rabi frequencies as were discussed in Secs. III A 1, III A 2, and III A 3. In each case, the spectrum has the same general shape as for the π-polarized probe. However, the EIA peaks in Figs. 13(a) and 13(c) are less prominent than those in Figs. 2 and 6. In both cases where the pump is more intense than the probe, the $g_5 \rightarrow e_5$ gives an important contribution [see Figs. 13(b) and 13(f)]. However, in the case where $\Omega_1/\Gamma = 0.5$ and $\Omega_2/\Gamma = 0.1$, the $g_1 \rightarrow e_1$ contribution, which has a dip at line center, is also important. This occurs because the pump is not intense enough to sweep the population completely over to the right and, indeed, all the other transitions give similar, smaller contributions to the total. When $\Omega_1/\Gamma = \Omega_2/\Gamma = 0.1$, we see from Fig. 13(d) that the $g_i \rightarrow e_i$, $i = 1-3$, transitions give the main contributions to the spectrum. This is quite

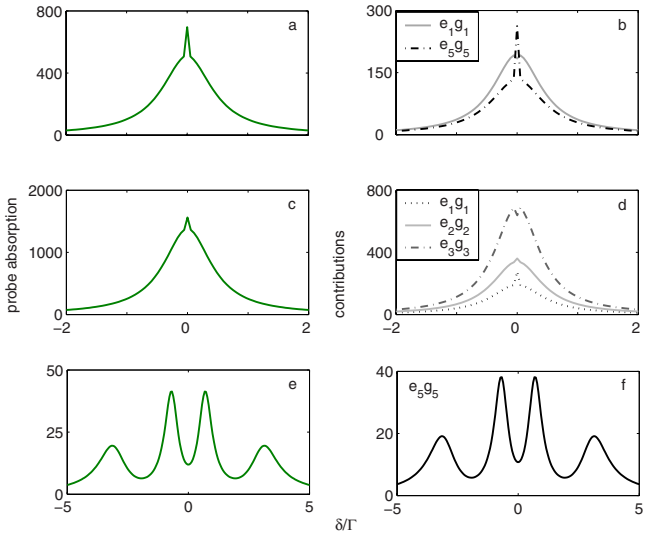

FIG. 13. (Color online) Probe absorption spectrum as a function of δ/Γ for interaction of an $F_g=2\rightarrow F_e=3$ transition with σ_+-polarized pump and σ_--polarized probe lasers: (a) total probe absorption for $\Omega_1/\Gamma=0.5$, $\Omega_2/\Gamma=0.1$; (b) main contributions to spectrum in (a) from $g_i\rightarrow e_i$, $i=1,5$, transitions; (c) total probe absorption for $\Omega_1/\Gamma=\Omega_2/\Gamma=0.1$; (d) main contributions to spectrum in (c) from $g_i\rightarrow e_i$, $i=1-3$, transitions; (e) total probe absorption for $\Omega_1/\Gamma=10$, $\Omega_2/\Gamma=0.6$; (f) main contribution to spectrum in (e) from $g_5\rightarrow e_5$ transition. $\gamma/\Gamma=0.001$ and the absorption and its contributions are in units of cm^{-1}.

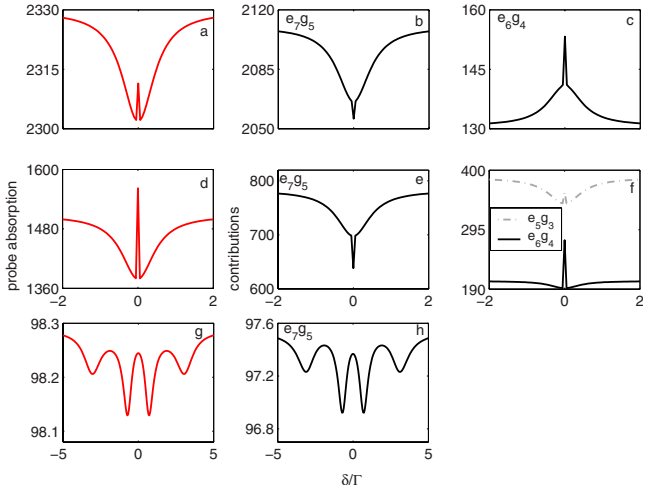

FIG. 14. (Color online) Pump absorption spectrum as a function of δ/Γ for interaction of an $F_g=2\rightarrow F_e=3$ transition with σ_+-polarized pump and σ_--polarized probe lasers: (a) total pump absorption for $\Omega_1/\Gamma=0.5$, $\Omega_2/\Gamma=0.1$; (b) and (c) main contributions to spectrum in (a) from $g_i\rightarrow e_{i+2}$, $i=5,4$, transitions; (d) total pump absorption for $\Omega_1/\Gamma=\Omega_2/\Gamma=0.1$; (e) and (f) main contributions to spectrum in (d) from $g_i\rightarrow e_{i+2}$, $i=5;3,4$, transitions; (g) total pump absorption for $\Omega_1/\Gamma=10$, $\Omega_2/\Gamma=0.6$; (h) main contribution to spectrum in (g) from $g_5\rightarrow e_7$ transitions. $\gamma/\Gamma=0.001$ and the absorption and its contributions are in units of cm^{-1}.

different from the situation when the probe is π polarized [see Fig. 6] where the transitions $g_i\rightarrow e_{i+1}$, $i=3-5$, give the main contributions.

The corresponding pump absorption spectra and their main contributions are plotted in Fig. 14 for the three cases shown in Fig. 13. We see that, in all the cases, the pump spectra have the same general shape as in the case of the π-polarized probe. Consequently, the same relationships between the pump and probe spectra found for the π-polarized probe hold for the σ_- probe. We see from Figs. 14(d) and 14(f), that when $\Omega_1>\Omega_2$, the same transitions contribute to the pump absorption as in the case of the π-polarized probe. Thus when the σ_+-polarized pump is stronger than the probe, the tendency is for the population to be swept to the right, regardless of whether the probe is π or σ_- polarized. This is also true (apart from $\delta\approx 0$) when the pump and probe are equally strong, and the probe is π polarized. However, when the probe is σ_- polarized, the probe tends to push the population toward the left in Fig. 1(b) whereas the pump tends to push it toward the right. This accounts for the main contributions to the probe spectrum coming from the left-hand transitions whereas the main contributions to the pump spectrum come from the right-hand transitions. A detailed analysis of the contributions to each of the pump and probe spectra, in the presence and absence of TOC, leads to conclusions that are similar to those for the π-polarized probe, except that, as shown in Eqs. (17) and (18), the relevant coherences are now between next-nearest neighbors.

IV. CONCLUSIONS

We have developed a general theory for the interaction of an $F_g\rightarrow F_e=F_g+1$ alkali-metal transition with an arbitrarily strong pump and probe that are perpendicularly polarized to each other with either $\sigma_\pm$ or π polarizations. We have shown that, when the pump is $\sigma_\pm$ polarized and the probe π polarized, or vice versa, the pump and probe absorption depend on the Zeeman coherences between the nearest-neighboring ground or excited Zeeman sublevels, whereas when the pump is σ_+ polarized and the probe σ_- polarized, or vice versa, the Zeeman coherences that directly determine the absorption are between next-nearest neighbors. In both cases, these coherences oscillate at frequencies $\pm\delta$, and are themselves determined by higher-order coherences at frequencies $\pm n\delta$. In this paper, the theory is applied to the specific case of the pump and probe absorption spectra for the degenerate $F_g=2\rightarrow F_e=3$ transition in the D_2 line of ^{87}Rb, interacting with a σ_+-polarized pump and either a π- or a σ_--polarized probe.

For the case of a π-polarized probe, we present detailed results for $\Omega_1>\Omega_2$ with $\Omega_1<\Gamma$ and $\Omega_1>\Gamma$, and $\Omega_1=\Omega_2$ with $\Omega_1<\Gamma$ and $\Omega_1>\Gamma$. The total pump and probe absorption spectra have been analyzed in terms of the contributions from the individual $g_i\rightarrow e_{i+1}$ probe and $g_i\rightarrow e_{i+2}$ pump transitions. In addition, each individual absorption spectrum has been analyzed according to the contributions from the populations and coherences of the ground- and excited-state Zeeman sublevels.

When $\Omega_1>\Omega_2$, the population is swept to the right, and the system can be approximated as an N-shaped system that is composed of a Λ and a V system. Both the probe absorp-

tion spectrum and the pump spectrum that derive from the Λ system have similar shapes, whereas the pump spectrum that derives from the V system has a shape complementary to theirs. When $\Omega_1 < \Gamma$, the probe absorption spectrum has an EIA peak at line center, and the pump absorption spectrum resembles that of the Λ system at line center and the V system in the wings. Thus, the pump and probe spectra are both characterized by an EIA peak at line center and complementary behavior in the wings. When $\Omega_1 > \Gamma$, the probe spectrum consists of four peaks at frequencies that can be calculated from the dressed states. The pump spectrum is mostly determined by the V system, and is therefore the mirror image of the probe spectrum.

When $\Omega_1 = \Omega_2$, all the individual transitions contribute to some extent to the total spectra. The contributions to the left of the energy-level scheme are usually characterized by EIT dips whereas those on the right have EIA peaks, and their relative weights determine whether the total spectrum has a peak or dip. Essentially, the inner transitions behave like a series of Λ systems, characterized by EIT dips at line center, in both the pump and probe spectra. However, both the ground- and excited-state populations are swept toward the right for these polarizations, so that the excited-state coherence, although small, also increases toward the right, resulting in EIA-type spectra. The same relation between the pump and probe spectra holds as before: for weak Rabi frequencies, both spectra have an EIA peaks at line center and complementary behavior in the wings, whereas for strong Rabi frequencies, the probe spectrum has a central dip and the pump spectrum shows complementary behavior.

From an analysis of the contributions to the individual probe and pump spectra, we find for weak Rabi frequencies that the sign of the contribution from the real part of the ground-state Zeeman coherence determines whether the spectra are characterized by an EIA peak (positive sign) or an EIT dip (negative sign). We confirm that TOC has the effect of making the coherence contribution less negative or even positive, thereby turning a sharp dip into a positive sharp peak. The central features are ultranarrow due to the long-lived ground-state Zeeman coherences. When the Rabi frequencies are strong, the ultranarrow features no longer appear due to the strong coupling of the ground and excited states, which tends to shorten the lifetime of the ground-state coherence [11]. An analysis of the contributions to the individual probe and pump spectra must include the real and imaginary parts of the ground- and excited-state Zeeman coherences and the populations. Here, we find that the coherences have the same general shape in the absence or presence of TOC, but the peaks and dips near line center are sharper in the presence of TOC.

For the case of a σ_+ pump and σ_- probe, the spectra have the same general shapes as for a σ_+ pump and π-polarized probe. When the pump is stronger than the probe, the main contributions to the spectrum come from the transitions toward the right, although the most extreme probe transition to the left may contribute when the pump is very weak. However, when both fields are equally strong, the transitions to the left determine the probe spectrum whereas those to the right determine the pump spectrum.

[1] H. Friedmann and A. D. Wilson-Gordon, Phys. Rev. A **36**, 1333 (1987).

[2] S. Hochman, A. D. Wilson-Gordon, and H. Friedmann, Opt. Lett. **15**, 631 (1990).

[3] C. Goren, A. D. Wilson-Gordon, M. Rosenbluh, and H. Friedmann, Phys. Rev. A **69**, 053818 (2004).

[4] A. M. Akulshin, S. Barreiro, and A. Lezama, Phys. Rev. A **57**, 2996 (1998).

[5] A. Lezama, S. Barreiro, and A. M. Akulshin, Phys. Rev. A **59**, 4732 (1999).

[6] A. V. Taichenachev, A. M. Tumaikin, and V. I. Yudin, Phys. Rev. A **61**, 011802(R) (1999).

[7] C. Goren, A. D. Wilson-Gordon, M. Rosenbluh, and H. Friedmann, Phys. Rev. A **67**, 033807 (2003).

[8] L. Spani Molella, R.-H. Rinkleff, and K. Danzmann, Phys. Rev. A **72**, 041802(R) (2005).

[9] A. J. Krmpot, M. M. Mijailovic, B. M. Panic, D. V. Lukic, A. G. Kovacevic, D. V. Pantelic, and B. M. Jelenkovic, Opt. Express **13**, 1448 (2005).

[10] R. Meshulam, T. Zigdon, A. D. Wilson-Gordon, and H. Friedmann, Opt. Lett. **32**, 2318 (2007).

[11] S. Boublil, A. D. Wilson-Gordon, and H. Friedmann, J. Mod. Opt. **38**, 1739 (1991).

[12] S. E. Harris, Phys. Today **50**(7), 36 (1997).

[13] F. Renzoni, W. Maichen, L. Windholz, and E. A. Arimondo, Phys. Rev. A **55**, 3710 (1997).

[14] A. D. Wilson-Gordon and H. Friedmann, Opt. Lett. **14**, 390 (1989).

[15] A. D. Wilson-Gordon, Phys. Rev. A **48**, 4639 (1993).

[16] H. Friedmann and A. D. Wilson-Gordon, Chem. Phys. Lett. **64**, 337 (1979).

[17] R. W. Boyd, *Nonlinear Optics*, 2nd ed. (Academic, San Diego, 2003).

[18] T. Zigdon, A. D. Wilson-Gordon, C. Goren, M. Rosenbluh, and H. Friedmann, Proc. SPIE **6604**, 660401 (2007).